European Journal of Neuroscience, Vol. 20, pp. 2251–2259, 2004

Nitric oxide synthase inhibition prevents neuronal death in the developing visual cortex

Yueting Zhang, Jie Zhang and Baolu Zhao
Laboratory of Visual Information Processing, Institute of Biophysics, Chinese Academy of Sciences, 15 Datun Road, ChaoYang District, Beijing 100101, People's Republic of China

Keywords: golden hamster, NADPH-d, postnatal development, TUNEL

Abstract

During postnatal development of the visual cortex of golden hamster, there is a transient increase in both the expression and the activity of nitric oxide synthase (NOS), which coincides temporally with the formation of ipsilateral retino-collicular and retino-geniculate projections and the functional differentiation of primary visual cortex, suggesting the involvement of NO in the maturation of the visual cortex. In the present study, an inhibitor of NOS, *N*-nitro-L-arginine (L-NNA) was used to block the NOS activity of newborn golden hamster, and effects on development were examined. L-NNA treatment caused an increase in mortality, and suppression of both body weight gain and nicotinamide adenine dinucleotide phosphate-diaphorase (NADPH-d) activity in the early phase of treatment (before postnatal day 14, PD14). The growth of NADPH-d-positive neurons in the visual cortex was also suppressed by the treatment. In control animals, significant numbers of apoptotic neurons were detected by terminal deoxynucleotidyl transferase-mediated dUTP nick end labelling assay on PD14, and this apoptosis mainly affected cells in cortical layers II and III. NOS inhibition largely rescued neurons from undergoing apoptosis, indicating that NO may serve as a signal triggering apoptosis and play a role in the maturation of the visual cortex.

Introduction

Apoptosis is generally accepted to play an important role in the regulation of neuronal types and numbers during development of the central and peripheral nervous systems (Naruse & Keino, 1995). At temporally distinct periods of development, cells that have been either produced in excess or completed their functional roles are eliminated, thus leading to the formation of mature brain circuits.

As a retrograde messenger, the developmental role of nitric oxide (NO) has been widely discussed in the nervous system. NO has been shown to influence neurotransmitter release and synaptogenesis, and modulate synaptic plasticity (reviewed by Contestabile, 2000), indicating that NO may play an important role in the development, maintenance and regulation of brain circuits. Several *in vitro* studies have shown both nutritive and toxic effects of NO in the survival of neurons (Estevez *et al*., 1998; Virgili *et al*., 1999; Nucci *et al*., 2003). However, conclusive data suggesting a role for NO in the survival of neurons during development are still lacking. Previous work has not shown a direct relationship between NO and neuronal apoptosis during development. No histopathological abnormalities were detected in nitric oxide synthase (nNOS) knockout mice (Huang *et al*., 1993), and the number and morphological features of granule cells were not changed either by injection of NOS inhibitors or knockout of NOS genes (reviewed by Contestabile, 2000). In addition, the apoptosis of dopaminergic neurons in the substantia nigra pars compacta (SNc) could not be blocked or attenuated by injection of N^{ω}-nitro-L-arginine methyl ester (L-NAME) or 7-nitroindazole (7-NI) (nNOS-specific inhibitors; Groc *et al*., 2002), while NOS inhibition also did not affect the survival of midbrain transplants in the striatum of rats (Van Muiswinkel *et al*., 1998). It is therefore still an open question as to whether NO functions in modulating neuronal apoptosis during the development of the nervous system.

The golden hamster (*Mesocricetus auratus*) is an ideal model for studying the development of the visual system. It has a short gestation and at birth is more immature than rats and mice, thus facilitating investigation of the early developmental events of the visual system. Our previous study has shown that, during postnatal development of golden hamster, there is a transient increase in both the level of enzyme and the activity of NOS in the visual cortex (Zhang *et al*., 2002). This increase coincides temporally with the formation of ipsilateral retino-collicular and retino-geniculate projections and the functional differentiation of primary visual cortex. In the present study, we used *N*-nitro-L-arginine (L-NNA) to block the activity of NOS and studied the effects of NOS inhibition on the development of visual cortex by means of nicotinamide adenine dinucleotide phosphate-diaphorase (NADPH-d) histochemistry and terminal deoxynucleotidyl transferase-mediated dUTP nick end labelling (TUNEL) assay.

Materials and methods

Animals and drug treatments

Golden hamsters used were from the breeding colony at the Institute of Epidemiology, Chinese Academy of Sciences. Animals received tap water and food *ad libitum*. All experimental procedures on live animals were performed under the supervision of a licensed veterinarian, according to guidelines based on NIH standards.

Twelve golden hamsters were studied at each time point, excluding animals suffering mortality. Within 24 h after birth was designated as the postnatal day 0 (PD0) and animals at PD3, PD7, PD14, PD21 and PD28 were examined. From PD1, pups were injected subcutaneously

Correspondence: Professor B. Zhao, as above.
E-mail: Zhaobl@sun5.ibp.ac.cn

Received 8 May 2004, revised 24 July 2004, accepted 22 August 2004

doi:10.1111/j.1460-9568.2004.03708.x

with 40 mg/kg/day L-NNA (Cramer *et al*., 1996; Vercelli *et al*., 2000), dissolved in saline, until the day on which the animals were killed. Control pups received an equivalent volume of saline only. Samples were collected 10–12 h after the last administration of L-NNA or saline. Mortality was monitored because it has been reported that NOS inhibition during development increases developmental mortality (Prickaerts *et al*., 1998).

NOS activity

Inhibition of NOS activity was examined using the electron spin resonance (ESR) technique, as previously reported (Zhang *et al*., 2002). Following decapitation, the visual cortex was isolated and homogenized in ice-cold suspension buffer [0.1 M NaCl, 0.01 M Tris/HCl (pH 7.6), 0.001 M EDTA (pH 8.0), 100 μg/mL PMSF, and a protease inhibitor cocktail tablet]. After centrifugation at 20 000 ***g*** for 30 min, the supernatant was collected and the total protein content was determined by Bradford method using BSA as standard. For ESR measurements, L-arginine, $CaCl_2$, NADPH, $Na_2S_2O_4$, diethyldithiocarbamate (DETC) and $FeSO_4$ were added to 1 mL of the homogenate supernatant of visual cortex to a final concentration of 500 μM L-arginine, 500 μM Ca^{2+}, 800 μM NADPH, 10 mM $Na_2S_2O_4$, 5 mM DETC and 1 mM Fe^{2+}. After incubation for 1.5 h at 37 °C, the solution was added to 1 : 5 of a volume of ethyl acetate to extract the $(DETC)_2$–Fe^{2+}–NO complex, shaken for 5 min, and then centrifuged at 6000 ***g*** for 12 min at room temperature. The upper layer of organic solvent was separated and kept for further applications in the dark at 4 °C. ESR spectra were recorded in a quartz tube at room temperature with an ER-200 spectrometer (Bruker, Germany) operating at X-band with 100 kHz modulation. The other parameters were: modulation amplitude 3.2G, microwave power 20 mW, central magnetic field 3380 G with scan 400 G, time constant 0.3 s and scan time 4 min. Each test was repeated three times.

Tissue preparation for microscopic analysis

Animals were given ether (PD3) or an overdose of sodium pentobarbitone (PD7 onwards) and perfused transcardially with 0.85% saline followed by 4% paraformaldehyde in 0.1 M phosphate buffer (PB, pH 7.4). The caudal third of the brain was dissected out, post-fixed in the same fixative for 3–5 h at 4 °C, and then immersed in 30% sucrose in PB at 4 °C. Coronal series sections, 20 μm thick, were cut with a cryostat microtome, and were divided into three series: one set of sections was underwent Nissl staining using cresyl violet (0.5%), one set of adjacent sections was collected for NADPH histochemical reactions, and the third adjacent set of sections was used for TUNEL assay.

NADPH-d histochemistry

NADPH-d co-localizes with NOS in the nervous system. Most neurons that exhibit NADPH-d activity, as tested by histochemistry, are also nNOS immunoreactive or have mRNA for nNOS (Bredt & Snyder, 1994). Thus, NADPH-d histochemistry is routinely used to reveal NOS-containing neurons and neurites.

After permeation for 30 min in a PBS solution containing 0.4% Triton X-100, NADPH-d activity was revealed by incubating the sections for 1 h at 37 °C in a PBS solution containing 0.1 mg/mL nitro blue tetrazolium and 1 mg/mL β-NADPH. Then, sections were rinsed for 15 min in PBS, dehydrated by exposure to graded ethanol rinses, dehydrated in xylene, mounted with colophony and examined by light microscopy.

Apoptosis

To quantify the number of apoptotic cells in the visual cortex, TUNEL assay was performed using an *in situ* cell apoptosis detection kit (Boster Biotech. Inc., Wuhan, China), as suggested by the manufacturer. Specificity of the DAB labelling was checked by omitting deoxynucleotidyl transferase from the working solution. All controls were uniformly negative. One section pretreated with DNAase I was used as a positive control.

Nuclei were also visualized using Hoechst 33258 and were examined for the typical features of apoptosis. Brain sections were re-hydrated, placed in Hoechst 33258 (5 μg/mL) for 20 min, then washed three times for 5 min each in PBS and mounted with an antifade mounting medium consisting of 90% glycerol in PBS, containing 1% p-phenylenediamine dihydrochloride (Sigma-Aldrich).

Data collection and statistical analysis

For NADPH-d and Nissl staining, 6–8 specific sections through lateral geniculate nucleus (LGN) or superior colliculus (SC) were examined. Both NADPH-d-positive and total cell numbers (observed at 40×) in area 17 were counted in columns spanning the whole cortical depth. Within each column, the ratio of NADPH-d-positive to total cells was normalized to 1000 cells. The size of NADPH-d-positive neurons was analysed using a Camera Lucida. For TUNEL assay, two sections through LGN or SC, respectively, were observed. Apoptosis was quantified by counting TUNEL-positive neurons in ten random fields of sections in each age group.

Results are expressed as the mean ± SD. Statistical analysis was performed using Student's *t*-test or one-way ANOVA as appropriate, and $P < 0.05$ was considered to indicate a significant difference.

Results

Effect of L-NNA treatment on mortality and body weight

During L-NNA treatment, the mortality of golden hamster pups was clearly increased (41.18% vs. 14.26% for control). The growth of pups was also suppressed in the first 2 weeks following the onset of treatment to inhibit NOS activity, as shown by their significant lower body weight compared with that of controls (3.96 g vs. 3.49 g on PD3, 7.39 g vs. 5.86 g on PD7). At PD14, two different responses were observed in L-NNA-treated animals: one group of animals exhibited severely hampered growth, and these animals died in the following week, whereas growth in the second group of animals increased up to that of controls (Fig. 1).

Effect of L-NNA treatment on NOS activity

The presence of NOS activity was detected by ESR spin trapping in the visual cortex of all age points of control animals, and typical ESR spectra are shown in Fig. 2. Chronic L-NNA treatment significantly reduced brain NOS activity. No typical NO signal was detected on PD3, PD7 and PD14 in L-NNA-treated animals. By PD21, NOS activity rose to 23.33% of control values (Fig. 2), and increased to 40.99% at PD28 (Table 1).

Effect of L-NNA treatment on development of NADPH-d-positive neurons

NADPH-d-positive neurons were detected in area 17 of the visual cortex in control and L-NNA animals on PD3, and these could be

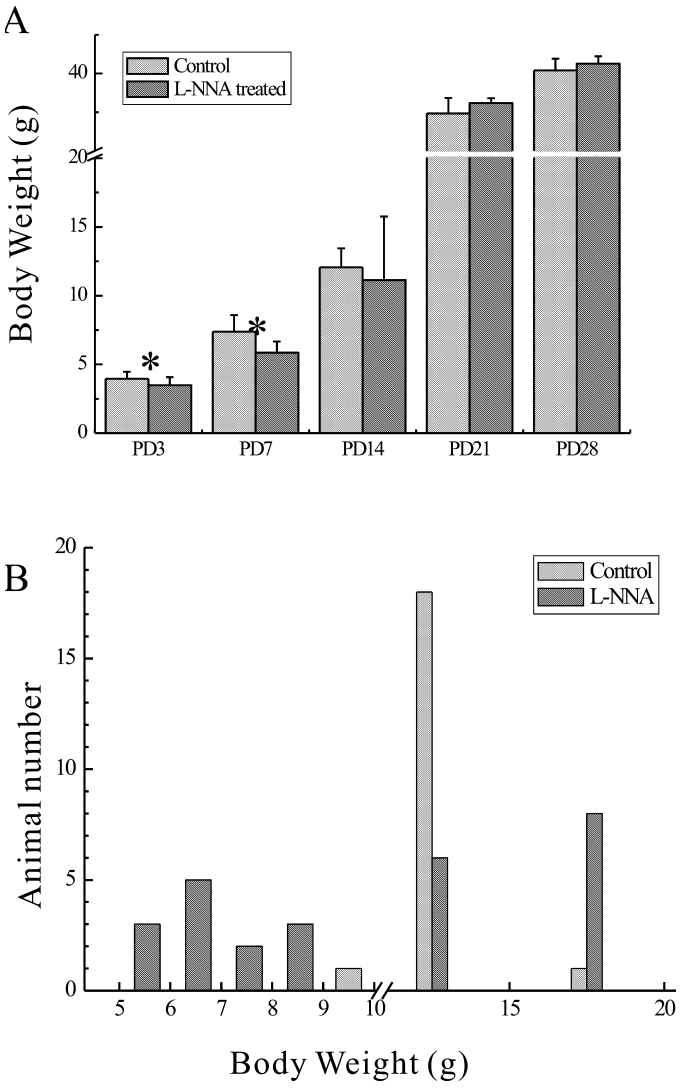

FIG. 1. Body weight from both control and L-NNA-treated golden hamsters. L-NNA treatment affected the gross development of newborns (PD3 and PD7), and these differences between control and treated groups disappeared from PD14 onwards (A). At PD14, pups treated with L-NNA could be divided into two groups (B): one group that failed to gain weight, and a second group in which weight gain increased to that of controls. *$P < 0.05$ (*t*-test), compared with controls of the same age. For all groups, $n \geq 6$.

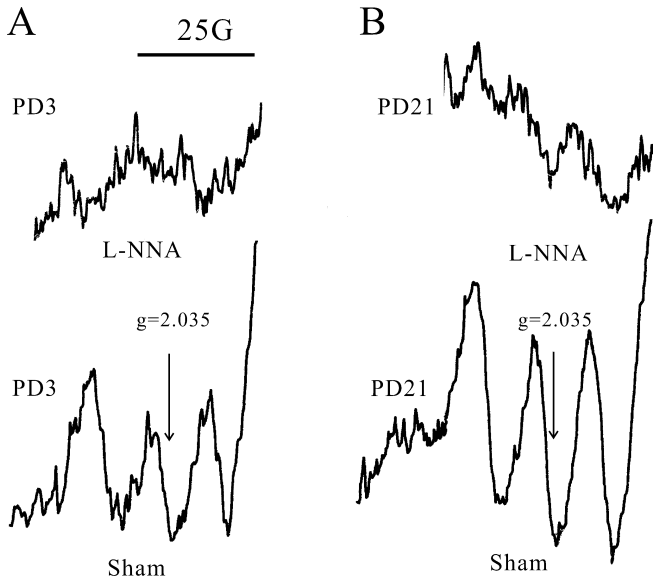

FIG. 2. Representative ESR spectra of NO signal from visual cortex of golden hamsters on PD3 (A) and PD21 (B) and the inhibitory effect of L-NNA on the signals. The ESR conditions are described in the Materials and Methods section. 25G, magnetic field in Gauss; g = 2.035, the ***g*** value of the ESR spectrum for spin-trapped NO-free radicals, as explained in the Materials and methods section.

divided into two types: the first was characterized by a darkly stained cell body and dendrites, and was mainly distributed in layers IV, V and VI and white matter, whereas the second type possessed a weakly stained cell body that was evenly distributed in all layers. Because of the large numbers and light staining of the latter, it was hard to quantify them. In this study, only the darkly stained neurons were analysed. On PD3, most NADPH-d-positive neurons presented in layer V/VI and white matter. Although no positive neurons were observed in the cortical plate, there were abundant positive fibres (Fig. 3A and B). Following L-NNA treatment, there was weaker background staining in the visual cortex, and significantly fewer NADPH-d-positive neurons were observed ($P < 0.05$).

More NADPH-d-positive neurons presented in the visual cortex on PD7 in both control and L-NNA-treated animals, and a few emerged in layer II/III (Fig. 3C). However, this increase was significantly reduced in L-NNA-treated groups compared with untreated controls ($P < 0.05$; Fig. 3D).

The density and distribution of NADPH-d-positive neurons on PD14 was almost the same as on PD7, but scattered positive neurons appeared in the superficial layer of the cortex (Fig. 3E and F). These cells were mainly multipolar neurons, although occasional bipolar neurons were also observed. At this time point, no significant difference in staining intensity and density of positive neurons was observed between L-NNA- treated and control groups.

On PD21, large numbers of NADPH-d-positive neurons emerged in the upper layers of the cortex. These neurons were abundant (about four- to five-fold greater numbers than in the deeper layers of the cortex), and were characterized by small numbers of dendrites, and by NADPH-d staining of moderate intensity (Fig. 3G and H). Interestingly, this appeared to be a new population of neurons, because the density of the typical darkly stained positive cells observed on PD14 was unchanged. NADPH-d-positive neurons were similarly detected in the upper layers of area 17 in L-NNA-treated groups, and no difference in their density and distribution was observed in treated animals compared with controls (Fig. 3G, H, K and L).

NOS activity in the upper layers of the visual cortex disappeared by PD28, but that of the deeper layers remained stable. Similar results

TABLE 1. Inhibition of NOS activity in visual cortex of golden hamster by L-NNA treatment. NOS activity is expressed as NO production (nmol/min/mg proteins). For every group, $n = 3$

	NO production (nmol/min/mg protein)	
Time	Sham group	L-NNA-treated group
PD 3	4.92 ± 0.26	Undetectable
PD 7	6.50 ± 0.68	Undetectable
PD14	8.41 ± 1.08	Undetectable
PD21	6.21 ± 0.66	1.45 ± 0.13
PD28	3.83 ± 0.26	1.57 ± 0.15

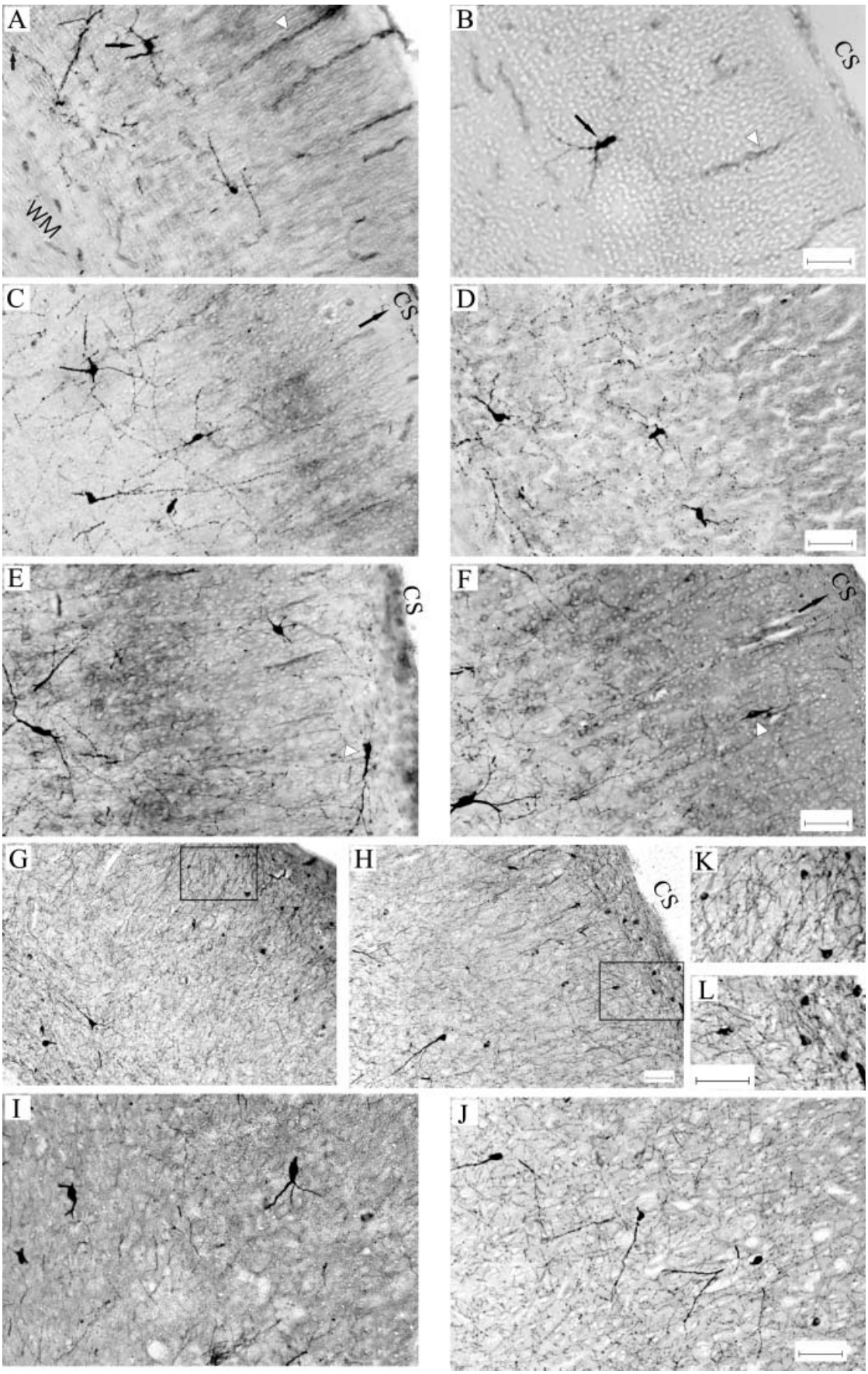
A
WM
B
CS
C
CS
D
E
CS
F
CS
G
H
CS
K
L
I
J

were gained from L-NNA-treated groups and untreated controls (Fig. 3I and J).

The size of NADPH-d-positive neuronal cell bodies in the visual cortex continuously increased after birth in both L-NNA-treated and untreated groups, and reached a peak at PD21 (from 506.27 ± 150.55 to 776.28 ± 167.52 μm^2 in controls, 383.92 ± 144.58 to 692.29 ± 173.95 μm^2 in L-NNA-treated animals), then remained stable (776.26 ± 213.74 and 645.02 ± 164.65 μm^2 for control and L-NNA-treated animals, respectively, at PD28). Interestingly, although L-NNA treatment was associated with a reduction in the numbers of NADPH-d-positive neurons in the early phase of development (see above, and Fig. 4B), it also led to a reduction in the size of these neurons. This difference in cell body size was significant at PD3, PD14, PD21 and PD28 (Fig. 4C; $P < 0.05$, one-way ANOVA).

Effect of L-NNA treatment on developmental apoptosis in area 17

Neuronal apoptosis was determined by *in situ* detection of DNA fragmentation as assessed using TUNEL assay. Using this technique, almost no apoptotic neurons were detected in area 17 on PD3 and PD7, either in L-NNA-treated animals or in controls. By PD14, apoptotic neurons appeared in the visual cortex, mainly presenting in layers II and III, and restricted to area 17 (Fig. 5B and C). This developmental apoptosis was apparently rescued by inhibition of NOS activity, although it was not completely blocked (Fig. 5D). The numbers of apoptotic neurons in PD14 sections were quantified, and approximately 75% fewer apoptotic neurons were observed in sections from L-NNA-treated animals compared with controls (121.27 ± 39.36 per mm^2 in L-NNA-treated animals vs. 515.72 ± 27.36 per mm^2 in untreated controls). Both control and treated groups did not show neuronal apoptosis on PD21 and PD28 (representative data are shown in Fig. 5A).

Apoptosis detected was further confirmed by Hoechst 33258 staining, and a similar apoptotic profile was obtained. Using this technique, significantly fewer apoptotic nuclei were detected in PD14 sections from L-NNA-treated animals than from controls (Fig. 6).

Discussion

The results of our experiments show that developmental apoptosis of visual cortical neurons is largely rescued by inhibition of NOS activity. We found that treatment of neonatal animals with the NOS inhibitor L-NNA was associated with a significant reduction in the numbers of apoptotic neurons in area 17 of the visual cortex (on PD14), as well as with a reduction in NADPH-d activity (before PD14) and in the growth of NADPH-d-positive neurons. These data are significant because they demonstrate for the first time an *in vivo* correlation between NOS activity and developmental apoptosis. We suggest that our results are important for our understanding of the role of NO in the development of the nervous system, especially developmental neuronal apoptosis.

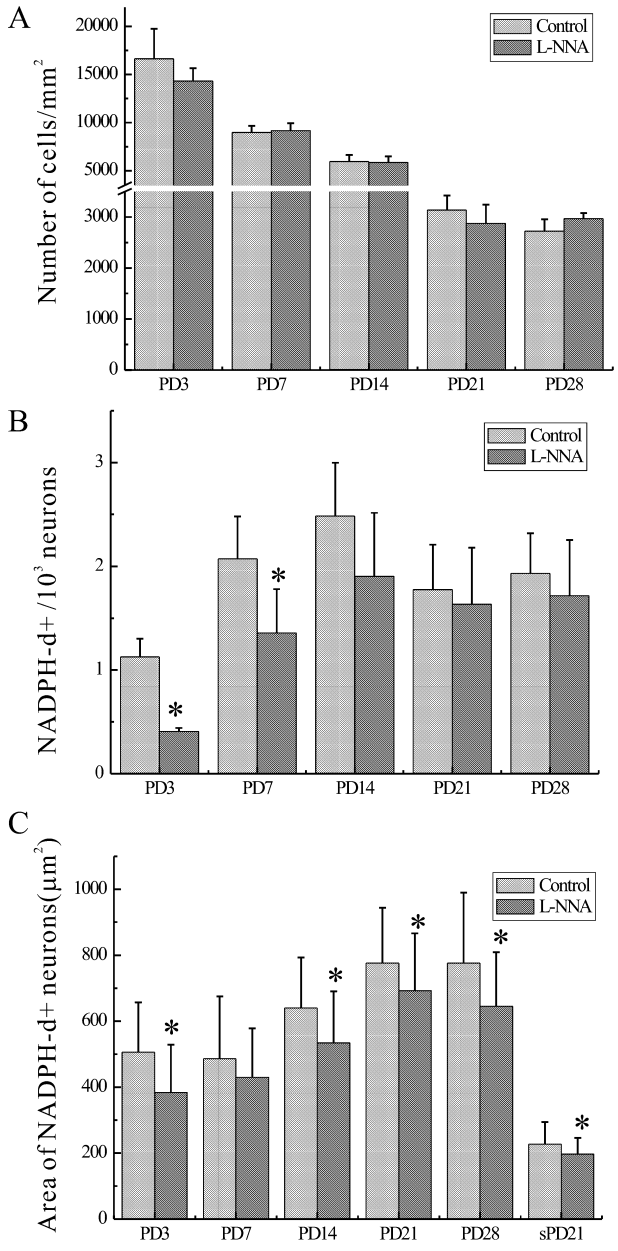

FIG. 4. The effect of L-NNA treatment on development of NADPH-diaphorase-positive neurons. (A) No effect on cell density in area 17 was detected after L-NNA treatment during postnatal development. (B) L-NNA affected the early development of NADPH-d-positive neurons in area 17. Significantly fewer NADPH-d-positive neurons were detected in L-NNA-treated samples on PD3 and PD7. (C) Growth of NADPH-d-positive neurons in area 17 of control and L-NNA-treated golden hamster. The body size of NADPH-d-positive neurons from L-NNA-treated groups was significantly smaller than that of controls on PD3, and from PD14 onwards (*$P < 0.05$, ANOVA). sPD21 represents NADPH-d-positive neurons observed transiently in the upper layers of area 17 on PD21 but not at other time points.

FIG. 3. NADPH-diaphorase staining in area 17 of controls (A, C, E, G, I) and L-NNA-treated (B, D, F, H and J) golden hamsters. (A and B) PD3. The long arrow indicates a darkly stained NADPH-d-positive neuron; short arrow, lightly stained NADPH-d-positive neuron; arrowhead, NADPH-d-positive fibre. (C and D) PD7. Significantly fewer NADPH-d-positive neurons and lighter background staining were observed in the L-NNA-treated group than in controls at PD3 and PD7 ($P < 0.05$). (E and F) PD14. NADPH-d-positive neurons were mainly observed in layers IV–VI and in sparse horizontal neurons (E) and bipolar neurons (F) scattered in the upper layers of the cortex (dark arrow). There was no significant difference in the total numbers of positive neurons and background staining in control and L-NNA-treated hamsters from PD14 onwards. (G and H) PD21. Many NADPH-d-positive neurons were observed in the upper layers of the cortex. Higher magnification characteristics of these neurons are shown in K and L, in control and L-NNA-treated samples, respectively. (I and J) PD28. NADPH-d-positive neurons in layers IV–VI. Positive neurons detected in the upper layers of the cortex on PD21 are no longer detectable. CS, cortical surface; WM, white matter. Scale bars, 100 μm.

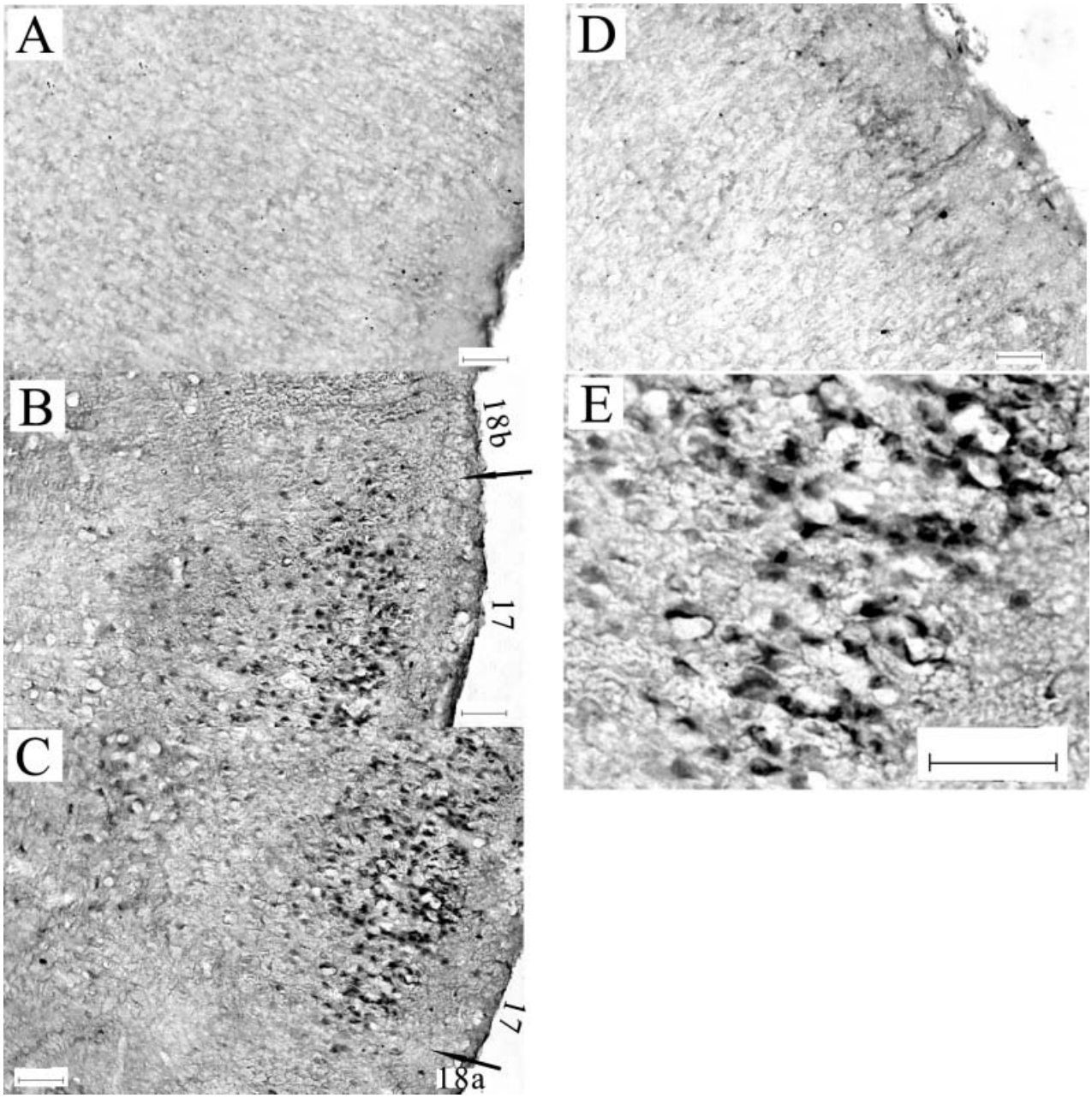

FIG. 5. Photomicrographs of apoptotic cells in area 17 of the developing golden hamster brain. No apparent apoptosis was detected on PD21 (A), or on PD3, PD7 or PD28 (data not shown). The upper layers of area 17 revealed substantial numbers of apoptotic neurons on PD14, and this phenomenon was restricted to area 17. Arrows indicate the border between areas 17–18b (B) and areas 17–18a (C). L-NNA treatment largely rescued neurons from apoptosis in area 17 on PD14 (D). High magnification in E reveals characteristic nuclear staining of labelled cells in area 17 on PD14 of control golden hamster. Scale bars, 100 μm.

The reduction in numbers of NADPH-d-positive neurons that we detected in our experiment following administration of NOS inhibitors was compatible with previous reports showing that NADPH-d and NOS activity co-localize in CNS neurons. For example, it has previously been reported that NOS and NADPH-d activities are simultaneously down-regulated by NOS inhibitors in the CNS (Paes de Carvalho *et al*., 1996), and that recovery of NADPH-d activity occurs in conjunction with recovery of NOS activity in rat brain (Virgili *et al*., 1999).

Although differences have been reported in the distribution of NOS activities among different areas of the brain, it has also been shown that NOS activity can be inhibited uniformly in different brain areas using intracerebroventricular administration of NOS inhibitors (Salter *et al*., 1995). In our study, neonatal animals received a 40 mg/kg injection of L-NNA from PD1. In the first 2 weeks of treatment, NOS activity in the region of interest was almost completely inhibited, whereas by the 3rd and 4th weeks, it rose to about 25–40% of control values. It is interesting to speculate that this increase may be due to a lower sensitivity to NOS inhibitors in older neonatal animals. In support of this hypothesis, similar results have been reported by a study investigating the role of NOS in the plasticity of rat somatosensory cortex (Sohn *et al*., 1999). The authors of that study similarly observed a rise of NOS activity after continual treatment using 20 mg/mL L-NNA for 4 and 6 weeks.

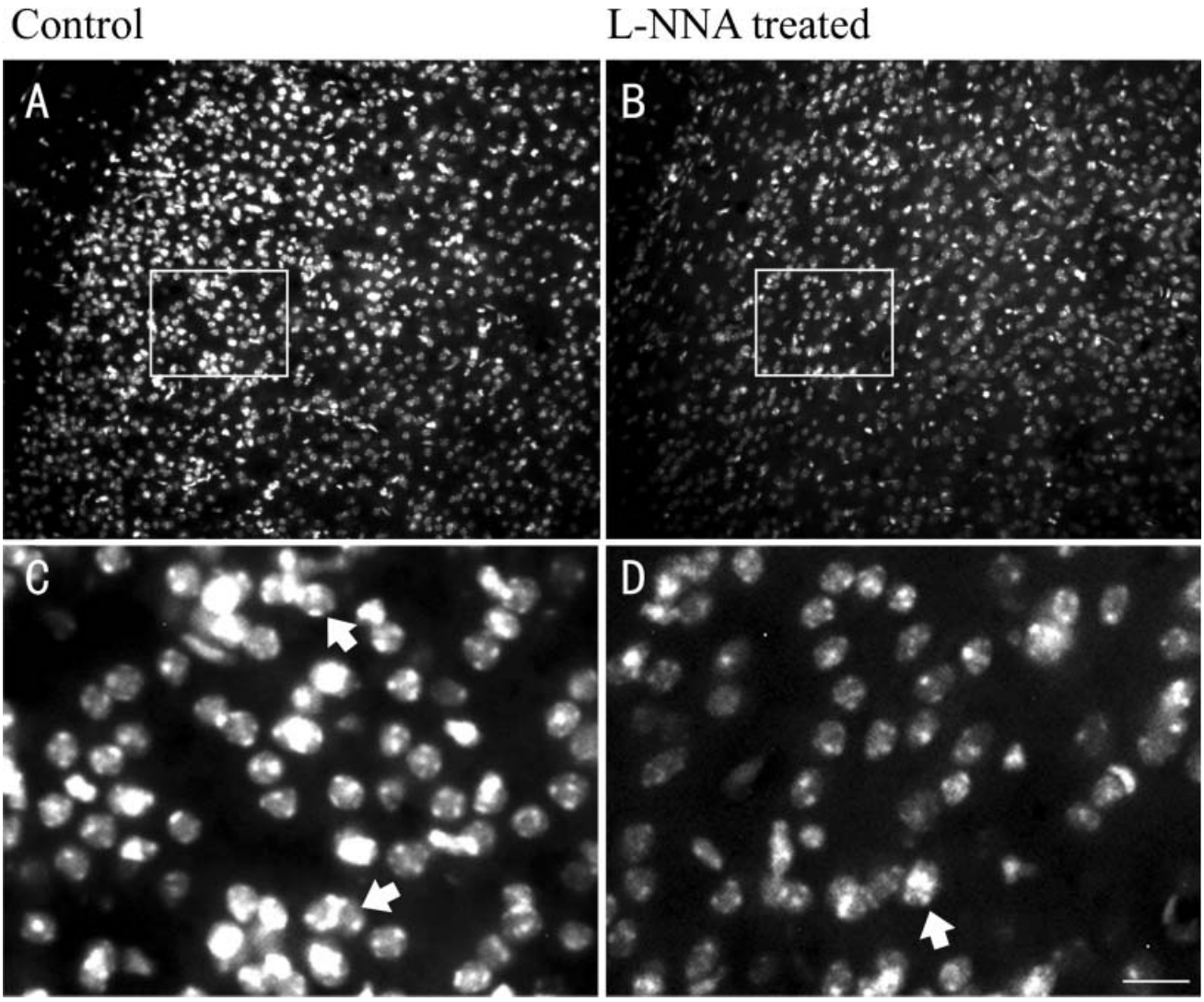

FIG. 6. Apoptotic cell profile in the golden hamster visual cortex as depicted with Hoechst 33258. Overview of sections from control (A) and L-NNA-treated (B) PD14 animal stained with Hoechst 33258. (C and D) Higher magnification of the frame area in A and C, respectively. Fragmented nuclei (arrows) are visible. Scale bars, 45 μm in A and B; 10 μm in C and D.

L-NNA and L-NAME are non-specific inhibitors for NOS, strongly inhibiting both nNOS and eNOS, whereas 7-NI is a more specific inhibitor of nNOS *in vivo*. Previous studies (Groc *et al*., 2002; Moreno-López *et al*., 2004) have used both L-NAME and 7-NI to study the effects of NOS blockade on neurogenesis and neuronal survival, and have reported no obvious differences in the effects observed using either of these two inhibitors. This may suggest that the source of the NO involved in neurogenesis and neuronal death during development is probably nNOS.

One of the most significant effects of disrupting neuronal NOS activity has been reported to be the development of a grossly enlarged stomach, and obstruction of gastric outflow (Voelker *et al*., 1995; Prickaert *et al*., 1998; Mashimo *et al*., 2000). We considered this as a potential cause of the suppression of body weight gain and increased mortality that we observed in our study. However, we feel that it was probably not the cause of these effects, because the reduction in body weight that we observed was transient, and recovery of body weight occurred while L-NNA treatment was still ongoing. Blood pressure elevation may be another outcome of NOS inhibition (Vercelli *et al*., 2000). However, previous studies suggest that the modulatory effects of NOS on development are not due to its regulation of blood pressure. For example, Vercelli *et al*. (2000) inhibited NOS activity by intraperitoneal injection of 40 mg/kg L-NNA, and did not detect any influence on neuronal projection patterns in the CNS despite the fact that the blood pressure in the brains of treated animals increased significantly.

Cell death is an important mechanism by which neuronal number is established in the nervous system. The majority of work investigating the relationship between NO and cell death has been performed *in vitro* (Van Muiswinkel *et al*., 1998). Groc *et al*. (2002) studied cell death and NOS activity in the SNc of rat but found no significant correlation, although variations in naturally occurring NOS activity were not reported in their study, and only the efficiency of NOS inhibition was examined. Based on their results, it is likely that NO does not participate in the maturation of SNc – in development, it has been demonstrated that a variety of signalling molecules influence cell survival, such as trophic factors and steroid hormones, along with other factors (Davies, 1994; Arai

et al., 1996). By contrast, in our study, which was performed in the visual cortex, we have found a clear correlation between the expression and activity of NOS and both developmental processes and cell death. Both the peak of NOS activity and neuronal apoptosis occurred on PD14, and inhibiting NOS rescued a significant percentage of these neurons. The differences between our results and previous reports may be due to the material used. The visual system of rats remains immature after birth (Lund *et al*., 1972; Blue & Parnavelas, 1983a,b; Naash *et al*., 1996). There is a rather long period before the formation of a stable neuronal population, and apoptosis occurs after a relatively prolonged phase of postnatal development. The visual cortex of golden hamsters is even more immature at birth. It has been reported that there is a peak in apoptosis on PD7 in the visual cortex of golden hamster, with almost all degenerating cells observed in external layers II and III (Finlay & Slattery, 1983). Our results show a similar laminar distribution of apoptotic cells, but the neuronal apoptosis was detected mainly on PD14, which is slightly later than that observed by Finlay & Slattery (1983). This minor difference may have been caused by the different methods used. For example, in their study, cell death was distinguished by observation of cresyl echt violet staining, whereas we used TUNEL staining. In the present study, most apoptotic neurons presented in layers II and III, most of which belong to the population of local circuit neurons possessing γ-aminobutyric acid (GABA) and peptide/calcium binding protein (Hendry *et al*., 1984; Papadopoulos *et al*., 1987). It has been reported that the subgroup of GABAergic neurons tends to undergo apoptosis, and that the number of peptidergic neurons decreases during the second half of the first postnatal month (Antonopoulos *et al*., 1992; Ferrer *et al*., 1992). The neuronal apoptosis detected in the present study coincided with the decrease in peptidergic neurons during development, while the neurochemical characters of these apoptotic neurons need further confirmation. We also observed inhibition of development of NADPH-d-positive neurons by L-NNA, and the long-term effect of this inhibition is now under investigation.

Neurogenesis is the other important mechanism controlling the development of the nervous system. Moreno-Lüpez *et al*. (2004) have demonstrated that NO has inhibitory effects on neurogenesis, and that NOS inhibition facilitates proliferation of progenitor cell in the subventricular zone of adult mice brain. In golden hamster, it has been reported that neurons in the visual cortex are produced on fetal day 10 to postnatal day 1 (Crossland & Uchwat, 1982). This precedes the period of NOS inhibitor administration in our study, although we cannot completely rule out effects of the inhibitor on the later stages of neurogenesis. This might be an interesting topic for future experiments to establish the balance between neurogenesis and apoptosis in our system, although such experiments would be beyond the scope of the current study.

In summary, neuronal apoptosis is spatially restricted within area 17 of golden hamster, and coincides with the formation of ipsilateral retino-collicular and retino-geniculate projections and the functional differentiation of primary visual cortex. We have found that NOS inhibition largely rescues neuronal apoptosis in area 17, suggesting that NO is involved in developmental apoptosis and perhaps participates in these physiological processes.

Acknowledgements

This work was supported by a grant from the National Natural Science Foundation of China. We thank Dr Gareth John (Mount Sinai School of Medicine, New York, USA) for his critical reading of the manuscript.

Abbreviations

DETC, diethyldithiocarbamate; ESR, electric spin resonance; LGN, lateral geniculate nucleus; NADPH-d, nicotinamide adenine dinucleotide phosphate-diaphorase; L-NNA, *N*-nitro-L-arginine; NO, nitric oxide; NOS, nitric oxide synthase; PD, postnatal day; SC, superior colliculus; SNc, substantia nigra pars compacta; TUNEL, terminal deoxynucleotidyl transferase-mediated dUTP nick end labelling.

References

Antonopoulos, J., Papadopoulos, G.C., Michaloudi, H., Cavanagh, M.E. & Parnavelas, J.G. (1992) Postnatal development of neuropeptide Y-containing neurons in the visual cortex of normal- and dark-reared rats. *Neurosci. Lett.*, **145**, 75–78.

Arai, Y., Sekine, Y. & Murakami, S. (1996) Estrogen and apoptosis in the developing sexually dimorphic preoptic area in female rats. *Neurosci. Res.*, **25**, 403–407.

Blue, M.E. & Parnavelas, J.G. (1983a) The formation and maturation of synapse in the visual cortex of the rat. I. Qualitative analysis. *J. Neurocytol.*, **12**, 599–616.

Blue, M.E. & Parnavelas, J.G. (1983b) The formation and maturation of synapse in the visual cortex of the rat. II. Qualitative analysis. *J. Neurocytol.*, **12**, 697–712.

Bredt, D.S. & Snyder, S.H. (1994) Nitric oxide: a physiologic messenger molecule. *Annu. Rev. Biochem.*, **63**, 175–195.

Contestabile, A. (2000) Role of NMDA receptor activity and nitric oxide production in brain development. *Brain Res. Brain Res. Rev.*, **32**, 476–509.

Cramer, K.S., Angelucci, A., Hahm, J.Q., Bogdanov, M.B. & Sur, M. (1996) A role for nitric oxide in the development of the ferret retinogeniculate projection. *J. Neurosci.*, **16**, 7995–8004.

Crossland, W.J. & Uchwat, C.J. (1982) Neurogenesis in the central visual pathways of the golden hamster. *Brain Res.*, **281**, 99–103.

Davies, A.M. (1994) Intrinsic programs of growth and survival in developing vertebrate nervous system. *Trends Neurosci.*, **17**, 195–199.

Estevez, A.G., Spear, N., Thompson, J.A., Cornwell, T.L., Radi, R., Barbeito, L. & Beckman, J.S. (1998) Nitric oxide-dependent production of cGMP supports the survival of rat embryonic motor neurons cultured with brain-derived neurotrophic factor. *J. Neurosci.*, **18**, 3708–3714.

Ferrer, J., Soriano, E., Del Rio, J.A., Alcantara, S. & Auladell, C. (1992) Cell death and removal in the cerebral cortex during development. *Prog. Neurobiol.*, **39**, 1–43.

Finlay, B.L. & Slattery, M. (1983) Local differences in the amount of early cell death in neocortex predict adult local specialization. *Science*, **219**, 1349–1351.

Groc, L., Hunter, T.J., Jiang, H., Bezin, L., Koubi, D., Corcoran, G.B. & Levine, R.A. (2002) Nitric oxide synthase inhibition during development: effect on apoptotic death of dopamine neurons. *Dev. Brain Res.*, **138**, 147–153.

Hendry, S.H.C., Jones, E.G., DeFelipe, J., Schmechel, D., Brandon, C. & Emson, P.C. (1984) Neuropeptides containing neurons in the cerebral cortex are also GABAergic. *Proc. Natl Acad. Sci. USA*, **81**, 6526–6530.

Huang, P.L., Dawson, T.M., Bredt, D.S., Snyder, S.H. & Fishman, M.C. (1993) Targeted disruption of the neuronal nitric oxide synthase gene. *Cell*, **75**, 1273–1286.

Lund, R.D. & Lund, J.S. (1972) Development of synaptic patterns in the superior colliculus of the rat. *Brain Res.*, **42**, 1–20.

Mashimo, H., Kjellin, A. & Goyal, R.K. (2000) Gastric stasis in neuronal nitric oxide synthase-deficient knockout mice. *Gastroenterology*, **119**, 766–773.

Moreno-López, B., Romero-Grimaldi, C., Noval, J.A., Murillo-Carretero, M., Matarredona, E.R. & Estrada, C. (2004) Nitric oxide is a physiological inhibitor of neurogenesis in the adult mouse subventricular zone and olfactory bulb. *J. Neurosci.*, **24**, 85–95.

Naash, M.L., Peachey, N.S., Li, Z.Y., Gryczan, C.C., Goto, Y., Blanks, J., Milam, A.H. & Ripps, H. (1996) Light-induced acceleration of photoreceptor degeneration in transgenic mice expressing mutant rhodopsin. *Invest. Ophthalmol. Visual Sci.*, **37**, 775–782.

Naruse, I. & Keino, H. (1995) Apoptosis in the developing CNS. *Prog. Neurobiol.*, **47**, 135–155.

Nucci, C., Piccirilli, S., Nistico, R., Morrone, L.A., Cerulli, L. & Bagetta, G. (2003) Apoptosis in the mechanisms of neuronal plasticity in the developing visual system. *Eur. J. Ophthalmol.*, **13** (Suppl. 3), S36–S43.

Paes de Carvalho, R., de Faria, M.H., do Nascimiento, J.L.M. & Hokoc, J.N. (1996) Development of NADPH-diaphorase in the avian retina regulation by

calcium ions and relation to nitric oxide synthase. *J. Neurochem.*, **67**, 1063–1071.

Papadopoulos, G.C., Parnavelas, J.G. & Cavanagh, M.E. (1987) Extensive co-existence of neuropeptides in the visual cortex. *Brain Res.*, **420**, 95–99.

Prickaerts, J., De Vente, J., Ittersum, M.M. & Steinbusch, H.W. (1998) Behavioural, neurochemical and neuroanatomical effects of chronic postnatal N-nitro-L-arginine methyl ester treatment in neonatal and adult rat. *Neurosci.*, **87**, 181–195.

Salter, M., Duffy, C., Garthwaite, J. & Strijbos, P.J. (1995) Substantial regional and hemispheric differences in brain nitric oxide synthase (NOS) inhibition following intracerebroventricular administration of N^{ω}-nitro-L-arginine (L-NA) and its methyl ester (L-NAME). *Neuropharmacology*, **34**, 639–649.

Sohn, N.W., Greenberg, J.H. & Hand, P.J. (1999) Chronic inhibition of NOS does not prevent plasticity of rat somatosensory (S1) cortex following deafferentation. *Brain Res.*, **816**, 396–404.

Van Muiswinkel, F.L., Drukarch, B., Steinbusch, H.W. & De Vente, J. (1998) Sustained pharmacological inhibition of nitric oxide synthase does not affect the survival of intrastriatal rat fetal mesencephalic transplants. *Brain Res.*, **792**, 48–58.

Vercelli, A., Garbossa, D., Biasiol, S., Repici, M. & Jhaveri, S. (2000) NOS inhibition during postnatal development leads to increased ipsilateral retinocollicular and retinogeniculate projection in rats. *Eur. J. Neurosci.*, **12**, 473–490.

Virgili, M., Monti, B., LoRusso, A., Bentivogli, M. & Contestabile, A. (1999) Developmental effects of in vivo and in vitro inhibition of nitric oxide synthase in neurons. *Brain Res.*, **839**, 164–172.

Voelker, C.A., Miller, M.J., Zhang, X.J., Eloby-Childress, S., Clark, D.A. & Pierce, M.R. (1995) Perinatal nitric oxide synthase inhibition retards neonatal growth by inducing hypertrophyic pyloric stenosis in rats. *Pediatr. Res.*, **38**, 768–774.

Zhang, Y.T., Zhang, D.L., Cao, Y.L. & Zhao, B.L. (2002) Developmental expression and activity variation of nitric oxide synthase in the brain of golden hamster: NOS in developing visual cortex. *Brain Res. Bull.*, **58**, 385–389.